SPARSITY-AIDED RADAR WAVEFORM SYNTHESIS

Heng Hu[*]*, Mojtaba Soltanalian*[†]*, Petre Stoica*[†] *and Xiaohua Zhu*[*]

[*] School of Electronic Engineering and Optoelectronics Techniques,
Nanjing University of Science and Technology, Jiangsu, China
[†] Dept. of Information Technology, Uppsala University, Uppsala, Sweden

ABSTRACT

Owing to the inherent sparsity of the target scene, compressed sensing (CS) has been successfully employed in radar applications. It is known that the performance of target scene recovery in CS scenarios depends highly on the coherence of the sensing matrix (CSM), which is determined by the radar transmit waveform. In this paper, we present a cyclic optimization algorithm to effectively reduce the CSM via a judicious design of the radar waveform. The proposed method provides a reduction in the size of the Gram matrix associated with the sensing matrix, and moreover, relies on the fast Fourier transform (FFT) operations to improve the computation speed. The effectiveness of the proposed algorithm is illustrated through numerical examples.

Index Terms— compressed sensing, mutual coherence, radar, sensing matrix, sparsity, waveform synthesis

1. INTRODUCTION AND SYSTEM MODELING

A primary interest in radar is the inverse problem of recovering the target scene from the noisy measurements. For a radar working under the conventional Nyquist-Shannon sampling framework, the sampling rate is constrained to be at least twice the highest frequency component in the received signal, in order to reconstruct the target scene accurately. In many cases, particularly for ultra wide band (UWB) radar, such a requirement is hardly achieved using the currently employed analog to digital converters (ADCs); not to mention the large computational burden caused by the processing of the data with high sampling rates.

The new framework of compressed sensing (CS) may promise a solution to such difficulties [1, 2]. To observe how, note that in practical radar applications, the target scene is typically sparse— i.e. there is usually a small number of targets that we are concerned with. In order to recover the data with lower sampling rates, CS relies on two criteria: (i) *sparsity*, which is related to the signal of interest (i.e. the target scene), and (ii) *incoherence*, which is related to the sensing modality to be designed. Note that CS-based formulations have been successfully developed for MIMO radar [4, 5], synthetic aperture radar (SAR) [6], as well as the inverse synthetic aperture radar (ISAR) [7].

In radar applications, the sensing modality is determined by the transmit sequence $\boldsymbol{s}$. The design problem can be formulated as follows. Suppose the target scene (in the range-Doppler plane) is discretized via a $N_r \times N_d$ grid, and define the time delay and Doppler shift matrices as

$$\boldsymbol{T}^r = \begin{pmatrix} \boldsymbol{0}_{r\times N} \\ \boldsymbol{I}_{N\times N} \\ \boldsymbol{0}_{(N_r-r-1)\times N} \end{pmatrix}, \qquad r = 0, 1, \cdots, N_r - 1, \tag{1}$$

$$\boldsymbol{F}^d = \begin{pmatrix} \omega_M^0 & 0 & \cdots & 0 \\ 0 & \omega_M^1 & \cdots & 0 \\ \vdots & \vdots & \ddots & \vdots \\ 0 & 0 & \cdots & \omega_M^{N-1} \end{pmatrix}^d, d = 0, 1, \cdots, N_d - 1,$$

where N is the length of transmit sequence $\boldsymbol{s}$, $\omega_M = e^{j\frac{2\pi}{M}}$ is the M^{th} root-of-unity. Thus, the discrete received signal can be formulated as (see [8–10] for details)

$$\boldsymbol{x} = \sum_{d=0}^{N_d-1} \sum_{r=0}^{N_r-1} \alpha_{r,d} \underbrace{\boldsymbol{T}^r \boldsymbol{F}^d \boldsymbol{s}}_{\triangleq \boldsymbol{\varphi}_{r,d}} + \boldsymbol{e} \tag{2}$$

where $\alpha_{r,d}$ denotes the complex scattering coefficient corresponding to the $(r,d)^{\text{th}}$ element of the grid, and $\boldsymbol{e}$ accounts for noise and all other unwanted interferences. Note that (2) can be recast in matrix form as

$$\boldsymbol{x} = \boldsymbol{\Phi}\boldsymbol{\alpha} + \boldsymbol{e} \tag{3}$$

where $\boldsymbol{\Phi} = (\boldsymbol{\varphi}_{0,0}, \boldsymbol{\varphi}_{0,1}, \ldots, \boldsymbol{\varphi}_{N_r-1,N_d-1})$ and $\boldsymbol{\alpha} = (\alpha_{0,0}, \alpha_{0,1}, \ldots, \alpha_{N_r-1,N_d-1})^T$. The goal of a radar system is to estimate the location, speed, and the radar cross-section (RCS) of the targets; in other words, to find the vector $\boldsymbol{\alpha}$ in the above equation. As discussed earlier, $\boldsymbol{\alpha}$ in (3) is usually sparse. Therefore, different methods from the CS literature can be used for designing $\boldsymbol{s}$ (equivalently an optimized sening matrix $\boldsymbol{\Phi}$), as well as to seek for the sparse $\boldsymbol{\alpha}$ in (3).

Notation: We use bold lowercase letters for vectors and bold uppercase letters for matrices. $(.)^T$ and $(.)^H$ denote the

This work was supported in part by the European Research Council (ERC), and the Swedish Research Council (VR).

vector/matrix transpose and the Hermitian transpose, respectively. $\mathbf{0}$ is the all-zero vector/matrix. $vec(\boldsymbol{X})$ is a vector obtained by stacking the columns of $\boldsymbol{X}$ successively. $\|\boldsymbol{x}\|_n$ or the l_n-norm of the vector $\boldsymbol{x}$ is defined as $(\sum_k |\boldsymbol{x}(k)|^n)^{\frac{1}{n}}$ where $\{\boldsymbol{x}(k)\}$ are the entries of $\boldsymbol{x}$. The Frobenius norm of a matrix $\boldsymbol{X}$ (denoted by $\|\boldsymbol{X}\|_F$) is equal to $\|vec(\boldsymbol{X})\|_2$. Finally, $\mathbb{C}$ represents the set of complex numbers.

2. MUTUAL COHERENCE

The mutual coherence, also known as the coherence of the sensing matrix (CSM) [12], is a useful metric to measure the incoherence required by CS, which can be defined as

$$\mu(\boldsymbol{\Phi}) \triangleq \max_{(r,d)\neq(r',d')} \frac{|\boldsymbol{\varphi}_{r,d}^H \boldsymbol{\varphi}_{r',d'}|}{\|\boldsymbol{\varphi}_{r,d}\|_2 \|\boldsymbol{\varphi}_{r',d'}\|_2}. \tag{4}$$

Suppose that the number of non-zero entries associated with the target scene $\tilde{\boldsymbol{\alpha}}$ satisfies the following inequality

$$\|\tilde{\boldsymbol{\alpha}}\|_0 < \frac{1}{2}\left(1 + \frac{1}{\mu(\boldsymbol{\Phi})}\right). \tag{5}$$

Then $\tilde{\boldsymbol{\alpha}}$ is necessarily the sparsest solution of the linear equation $\boldsymbol{x} = \boldsymbol{\Phi}\boldsymbol{\alpha}$. Moreover, fast greedy algorithms such as the basis pursuit (BP) or the orthogonal matching pursuit (OMP) are guaranteed to find the correct solution $\boldsymbol{\alpha}$ [2, 10]. A suitable approach to describe $\mu(\boldsymbol{\Phi})$ is via the Gram matrix $\boldsymbol{G} \triangleq \tilde{\boldsymbol{\Phi}}^H \tilde{\boldsymbol{\Phi}}$, where $\tilde{\boldsymbol{\Phi}}$ is the column-normalized version of $\boldsymbol{\Phi}$. Consequently, $\mu(\boldsymbol{\Phi})$ can be stated as

$$\mu(\boldsymbol{\Phi}) = \max_{k\neq l} \; |\boldsymbol{G}(k,l)| \tag{6}$$

where $\{|\boldsymbol{G}(k,l)|\}_{k\neq l}$ are the *coherence coefficients* associated with the sensing matrix $\boldsymbol{\Phi}$.[1]

Note that a matrix $\boldsymbol{\Phi}$ with low coherence corresponds to a Gram matrix $\boldsymbol{G}$ which is close to identity $\boldsymbol{I}$. As a result, one can reduce the incoherence conveniently via the optimization problem:

$$\min_{\boldsymbol{\Phi}} \; \|\boldsymbol{G} - \boldsymbol{I}\|_F^2. \tag{7}$$

Due to its quartic objective, (7) is deemed to be easier to tackle compared to (6); however, a large number of variables can make the problem prohibitive. In the next section, we will discuss a more effective approach that formulates a quadratic alternative of (7), and particularly facilitates using the fast Fourier transform (FFT) operations to tackle the problem.

3. WAVEFORM SYNTHESIS

Due to practical constraints, unimodular sequences are very desirable for transmission purposes [13]. As a result, we consider the design of a unimodular transmit sequence $\boldsymbol{s}$ (with $|\boldsymbol{s}(k)| = 1, \forall\, k$) in the following.

[1] We note that, according to the formulation in (2), the coherence coefficients can also be associated with the transmit sequence $\boldsymbol{s}$.

We begin the design formulation noting that the coherence between any two arbitrary columns of the matrix $\tilde{\boldsymbol{\Phi}}$ (and equivalently the corresponding element in the Gram matrix $\boldsymbol{G}$) can be written as

$$\begin{aligned}
\tilde{\boldsymbol{\varphi}}_{r,d}^H \tilde{\boldsymbol{\varphi}}_{r',d'} &= \left(\frac{1}{\sqrt{N}} \boldsymbol{T}^r \boldsymbol{F}^d \boldsymbol{s}\right)^H \left(\frac{1}{\sqrt{N}} \boldsymbol{T}^{r'} \boldsymbol{F}^{d'} \boldsymbol{s}\right) \\
&= \frac{1}{N}\left(\boldsymbol{s}^H \boldsymbol{F}^{d\,H} \boldsymbol{T}^{r\,H}\right)\left(\boldsymbol{T}^{r'} \boldsymbol{F}^{d'} \boldsymbol{s}\right) \\
&= \frac{1}{N} \boldsymbol{s}^H \boldsymbol{F}^{d\,H} \widetilde{\boldsymbol{T}}_{\Delta r} \boldsymbol{F}^{d'} \boldsymbol{s}
\end{aligned} \tag{8}$$

where $\widetilde{\boldsymbol{T}}_{\Delta r} = \boldsymbol{T}^{r H} \boldsymbol{T}^{r'}$, and $\Delta r = r' - r$. Based on the above equation, it is easy to verify that the terms formulated in (8) are identical for all (r, r') with the same Δr. Therefore, the Gram matrix $\boldsymbol{G}$ has a specific structure that can be exploited. Namely, using (8) the objective function in (7) can be rewritten as

$$\begin{aligned}
&\|\boldsymbol{G} - \boldsymbol{I}\|_F^2 \\
&= \left\| \begin{pmatrix} \widetilde{\boldsymbol{G}}_0 & \widetilde{\boldsymbol{G}}_1 & \cdots & \widetilde{\boldsymbol{G}}_{N_r-1} \\ \widetilde{\boldsymbol{G}}_{-1} & \widetilde{\boldsymbol{G}}_0 & \cdots & \widetilde{\boldsymbol{G}}_{N_r-2} \\ \vdots & \vdots & \ddots & \vdots \\ \widetilde{\boldsymbol{G}}_{1-N_r} & \widetilde{\boldsymbol{G}}_{2-N_r} & \cdots & \widetilde{\boldsymbol{G}}_0 \end{pmatrix} - \boldsymbol{I} \right\|_F^2 \\
&= \sum_{r=-(N-1)}^{N-1} \gamma_r^2 \, \|\widetilde{\boldsymbol{G}}_r - \boldsymbol{I}\delta_r\|_F^2
\end{aligned} \tag{9}$$

where

$$\widetilde{\boldsymbol{G}}_r = \boldsymbol{X}^H \widetilde{\boldsymbol{T}}_r \boldsymbol{X}, \tag{10}$$

$$\boldsymbol{X} = (\boldsymbol{x}_0, \boldsymbol{x}_1, \ldots, \boldsymbol{x}_{N_d-1}), \tag{11}$$

$$\boldsymbol{x}_d = \frac{1}{\sqrt{N}} \boldsymbol{F}^d \boldsymbol{s} \quad , \quad d = 0, 1, \ldots, N_d - 1, \tag{12}$$

$$\gamma_r^2 = \begin{cases} N_r - |r|, & |r| < N_r, \\ 0, & \text{otherwise}, \end{cases} \tag{13}$$

and δ_r denotes the Kronecker delta function:

$$\delta_r = \begin{cases} 1, & r = 0, \\ 0, & r \neq 0. \end{cases} \tag{14}$$

It is worth observing that (9) contributes a significant reduction in the size of the matrix variables.

Next note that $\widetilde{\boldsymbol{T}}_r$ is a shifting matrix, and hence $\widetilde{\boldsymbol{G}}_r$ can be viewed as the covariance matrix of the vectors $\{\boldsymbol{x}_d\}$ corresponding to the time lag r. Based on this observation, the

following Parseval-type equality holds [14]:

$$\|\boldsymbol{G}-\boldsymbol{I}\|_F^2 = \sum_{r=-(N-1)}^{N-1} \gamma_r^2 \|\widetilde{\boldsymbol{G}}_r - \boldsymbol{I}\delta_r\|_F^2 = \frac{1}{2N}\sum_{p=1}^{2N} \left\| \boldsymbol{\Psi}\left(\frac{2\pi p}{2N}\right) - \gamma_0 \boldsymbol{I} \right\|_F^2 \quad (15)$$

in which

$$\boldsymbol{\Psi}(\omega) = \sum_{r=-(N-1)}^{N-1} \gamma_r \boldsymbol{X}^H \widetilde{\boldsymbol{T}}_r \boldsymbol{X}\, e^{-j\omega r}. \quad (16)$$

Interestingly, the frequency domain criterion in (15) has the same form as (28) in [14]. Therefore, we employ a similar approach to tackle the problem herein. In particular, the $\boldsymbol{\Psi}(\omega)$ defined in (16) can also be written in the form

$$\boldsymbol{\Psi}(\omega) = \boldsymbol{Z}^H(\omega)\boldsymbol{\Gamma}\boldsymbol{Z}(\omega) \quad (17)$$

with

$$\boldsymbol{Z}(\omega) = (\boldsymbol{z}(1)e^{-j\omega}, \ldots, \boldsymbol{z}(N)e^{-j\omega N})^T, \quad (18)$$

$$\boldsymbol{z}(n) = (\boldsymbol{x}_0(n), \ldots, \boldsymbol{x}_{N_d-1}(n))^T \quad (19)$$

for $1 \le n \le N$, and

$$\boldsymbol{\Gamma} = \begin{pmatrix} \gamma_0 & \gamma_1 & \cdots & \gamma_{N-1} \\ \gamma_{-1} & \gamma_0 & \cdots & \vdots \\ \vdots & \vdots & \ddots & \gamma_1 \\ \gamma_{-N+1} & \cdots & \gamma_{-1} & \gamma_0 \end{pmatrix}. \quad (20)$$

As a result, we have that

$$\|\boldsymbol{G}-\boldsymbol{I}\|_F^2 = \frac{1}{2N}\sum_{p=1}^{2N} \|\boldsymbol{Z}_p^H \boldsymbol{\Gamma} \boldsymbol{Z}_p - \gamma_0 \boldsymbol{I}\|_F^2 \quad (21)$$

where $\boldsymbol{Z}_p \triangleq \boldsymbol{Z}(2\pi p/(2N))$. Now note that $\|\widetilde{\boldsymbol{G}}_0 - \boldsymbol{I}\|_F^2$ is a constant, and thus, a diagonal loading of $\boldsymbol{\Gamma}$ does not change the solution to (7). Let $\tilde{\boldsymbol{\Gamma}} = \boldsymbol{\Gamma} + \lambda \boldsymbol{I}$, with λ being a non-negative scalar that can ensure $\tilde{\boldsymbol{\Gamma}} \ge 0$. Consequently, one can reduce the incoherence of $\boldsymbol{\Phi}$ conveniently using the following quadratic alternative of (21):

$$\begin{aligned} \min_{\boldsymbol{s}, \boldsymbol{U}_p} \quad & \sum_{p=1}^{2N} \|\boldsymbol{C}\boldsymbol{Z}_p - \sqrt{\gamma_0}\boldsymbol{U}_p\|_F^2 \\ \text{s.t.} \quad & |\boldsymbol{s}_n| = 1, \qquad n = 1, \ldots, N, \\ & \boldsymbol{U}_p^H \boldsymbol{U}_p = \boldsymbol{I},\ p = 1, \ldots, 2N, \end{aligned} \quad (22)$$

where $\boldsymbol{C}$ is the Hermitian square root of $\tilde{\boldsymbol{\Gamma}}$, i.e. $\boldsymbol{C}^H\boldsymbol{C} = \tilde{\boldsymbol{\Gamma}}$.

To tackle the minimization problem in (22), we adopt a cyclic method as follows. For given $\{\boldsymbol{Z}_p\}_{p=1}^{2N}$ (equivalently a given transmit sequence $\boldsymbol{s}$), let $\boldsymbol{Z}_p^H \boldsymbol{C}^H = \boldsymbol{U}_1 \boldsymbol{\Sigma} \boldsymbol{U}_2^H$ represent the *economy-size* singular value decomposition (SVD) of $\boldsymbol{Z}_p^H \boldsymbol{C}^H$, with $\boldsymbol{U}_1$ being an $N_d \times N_d$ unitary matrix, $\boldsymbol{\Sigma}$ being an $N_d \times N_d$ diagonal matrix and $\boldsymbol{U}_2$ being an $N \times N_d$ semi-unitary matrix. Then the minimizer $\boldsymbol{U}_p$ of (22) is given by [14]

$$\boldsymbol{U}_p = \boldsymbol{U}_2 \boldsymbol{U}_1^H. \quad (23)$$

Similar to the WeCAN algorithm in [14], the computation of $\boldsymbol{C}\boldsymbol{Z}_p$ can be performed using the FFT operation. To observe how, let

$$\tilde{\boldsymbol{X}}_m = \boldsymbol{C}^T \odot (\boldsymbol{x}_m, \boldsymbol{x}_m, \ldots, \boldsymbol{x}_m)_{N\times N} \quad (24)$$

for $0 \le m \le N_d - 1$, and

$$\boldsymbol{F} = \sqrt{2N}\boldsymbol{A}^H \tilde{\boldsymbol{F}}, \quad \tilde{\boldsymbol{F}} = \begin{pmatrix} \tilde{\boldsymbol{X}}_0 & \cdots & \tilde{\boldsymbol{X}}_{N_d-1} \\ \boldsymbol{0}_{N\times N} & \cdots & \boldsymbol{0}_{N\times N} \end{pmatrix} \quad (25)$$

where $\boldsymbol{A}$ denotes the $2N \times 2N$ (inverse) DFT matrix, whose (l,p)-element is given by

$$[A]_{l,p} = \frac{1}{\sqrt{2N}} e^{j2\pi lp/(2N)}, \quad l,p = 1, \ldots, 2N. \quad (26)$$

Using the above formulations, one can observe that the $N \times N_d$ matrix $\boldsymbol{C}\boldsymbol{Z}_p$ may be obtained by reshaping the $NN_d \times 1$ vector $\boldsymbol{f}_p$ into each column of $\boldsymbol{C}\boldsymbol{Z}_p$, where $\boldsymbol{f}_p^T$ represents the p^{th} row of $\boldsymbol{F}$.

Next we discuss the minimization of (22) with respect to $\boldsymbol{s}$ for given $\{\boldsymbol{U}_p\}_{p=1}^{2N}$. Let

$$\boldsymbol{V}_{2N\times NN_d} = (\boldsymbol{v}_1, \boldsymbol{v}_2, \ldots, \boldsymbol{v}_{2N})^T \quad (27)$$

where $\boldsymbol{v}_p = \sqrt{\gamma_0}\ vec(\boldsymbol{U}_p)$, $1 \le p \le 2N$. Then the criterion in (22) can be written as

$$\sum_{p=1}^{2N} \|\boldsymbol{C}\boldsymbol{Z}_p - \sqrt{\gamma_0}\boldsymbol{U}_p\|_F^2 = \left\|\sqrt{2N}\boldsymbol{A}^H\tilde{\boldsymbol{F}} - \boldsymbol{V}\right\|_F^2 = 2N \left\|\tilde{\boldsymbol{F}} - \frac{1}{\sqrt{2N}}\boldsymbol{A}\boldsymbol{V}\right\|_F^2. \quad (28)$$

Note that (28) can be minimized with respect to each element of $\boldsymbol{s}$ in a separate manner. Particularly, we can consider minimizing the following criterion with respect to s (a generic element of $\boldsymbol{s}$):

$$\sum_{k=1}^{NN_d} |\mu_k s - \nu_k|^2 = \text{const} - 2\Re\left[\left(\sum_{k=1}^{NN_d} \mu_k^* \nu_k\right) s^*\right] \quad (29)$$

where $\{\mu_k\}$ are given by the elements of $\tilde{\boldsymbol{F}}$ that contain s, and ν_k is given by the element of $\frac{1}{\sqrt{2N}}\boldsymbol{A}\boldsymbol{V}$ whose position is the same as that of μ_k in $\tilde{\boldsymbol{F}}$. Hence, the unimodular s minimizing (29) is

$$s = e^{j\varphi},\ \varphi = \arg\left(\sum_{k=1}^{NN_d} \mu_k^* \nu_k\right). \quad (30)$$

Finally, the steps of the proposed algorithm for designing the transmit sequence $\boldsymbol{s}$ are summarized in Table 1.

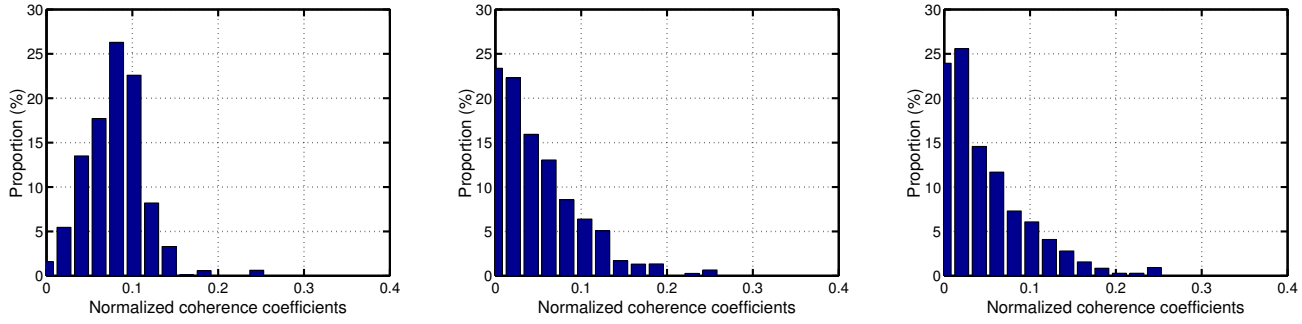

(a) (b) (c)

Fig. 1. Distribution of the coherence coefficients associated with (a) Alltop sequence, and (b-c) the optimized sequences obtained by the proposed method and the coherence reduction approach in [10], respectively, using the Alltop sequence as initialization.

Table 1. The Proposed Algorithm for Sparsity-Aided Transmit Sequence Design

Step 0: Initialize the transmit sequence $\boldsymbol{s}$ with a random unimodular sequence (or by a good existing sequence). Calculate the Hermitian square root $\boldsymbol{C}$ of $\tilde{\boldsymbol{\Gamma}}$.

Step 1: Fix $\boldsymbol{s}$ (equivalently $\{\boldsymbol{Z}_p\}_{p=1}^{2N}$) and compute $\{\boldsymbol{U}_p\}_{p=1}^{2N}$ using (23).

Step 2: Fix $\{\boldsymbol{U}_p\}_{p=1}^{2N}$ and compute $\boldsymbol{s}$ using (30).

Step 3: Repeat steps 1 and 2 until a stop criterion is satisfied, e.g. $\|\boldsymbol{s}^{(t+1)} - \boldsymbol{s}^{(t)}\|_F < \varepsilon$ for some given $\varepsilon > 0$, where t denotes the total iteration number.

4. NUMERICAL EXAMPLLES

4.1. Incoherence

We consider employing the proposed method to design a transmit sequence $\boldsymbol{s}$ of length $N = 127$, using the Alltop sequence as initialization, for a target scene with $N_r = 20$ range and $N_d = 15$ Doppler bins. The Alltop sequence is known to yield a desirable incoherence property of the sensing matrix $\boldsymbol{\Phi}$ [9], and is defined for prime lengths $N > 5$ as

$$\boldsymbol{s}(n) = e^{j\frac{2\pi}{N}n^3}, \quad n = 1, 2, \ldots, N. \tag{31}$$

In a type of example inspired by [10], we compare the coherence coefficients associated with the Alltop sequence, and those of the optimized sequence obtained by the proposed method. Furthermore, we include the results obtained by using the coherence reduction approach in [10] initialized by the Alltop sequence. The results are shown in Fig. 1. It can be observed from Fig. 1 that the proposed method in this work and the approach in [10] can lead to a similar coherence distribution. On the other hand, both methods outperform the Alltop sequence in terms of incoherence.

4.2. Target Scene Recovery

In order to verify the effectiveness of the optimized sequences, we examine the root mean-square errors (RMSEs) of the target scene recovery for different sparsity orders $K = \|\boldsymbol{\alpha}\|_0$. We construct the sparse vectors $\boldsymbol{\alpha}$ by choosing K non-zero locations in the vector, with identical chance for all $\binom{N_d N_r}{K}$ assignments of the non-zero locations, and consider random positive RCS values for the non-zero locations. We let $N = 127$, $N_r = 20$, $N_d = 15$, and set the signal-to-noise ratio to 20dB. Based on these settings, we use the OMP algorithm for the recovery of $\boldsymbol{\alpha}$. The results leading to Fig. 2 are obtained by averaging the computation times for 500 Monte Carlo experiments (with different random initializations). Once again, the proposed method and the approach in [10] present a very similar performance. However, according to Fig. 2, the optimized sequences obtained by both methods can yield a smaller RMSE compared to that of Alltop sequence; particularly when the sparsity order K grows large. We note that for larger values of K, a low incoherence of the sensing matrix $\boldsymbol{\Phi}$ becomes more crucial to an accurate reconstruction of the target scene; see (5).

4.3. Computation Time

Finally, we compare the computation times required by the proposed method and the coherence reduction approach devised in [10], when performing the sequence design for various lengths N of the transmit sequence. Herein, we set $M = 10$, $N_d = 8$, and $N_r = N$. It can be observed from Fig. 3 that the computation time of the design algorithm in [10] is growing rapidly as N grows large. In contrary, the proposed algorithm can be used for comparably large lengths of the transmit sequence, e.g. $N \gtrsim 100$. The results leading to Fig. 3 were obtained by averaging the computation times over 100 experiments (with different random initializations) using a PC with

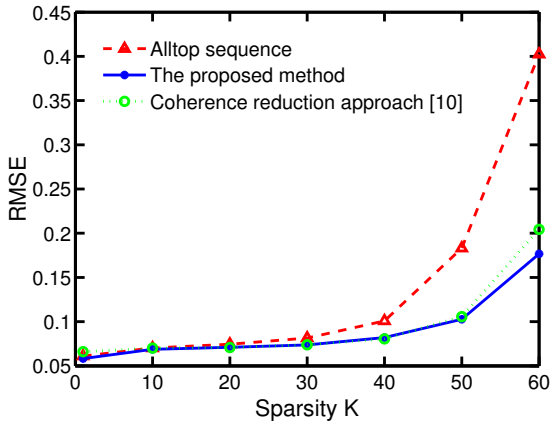

Fig. 2. Comparison of the recovery error for sensing matrices built based on the Alltop sequence and the optimized sequences obtained by the proposed method and the approach in [10], for different sparsity orders K of the target scene $\boldsymbol{\alpha}$.

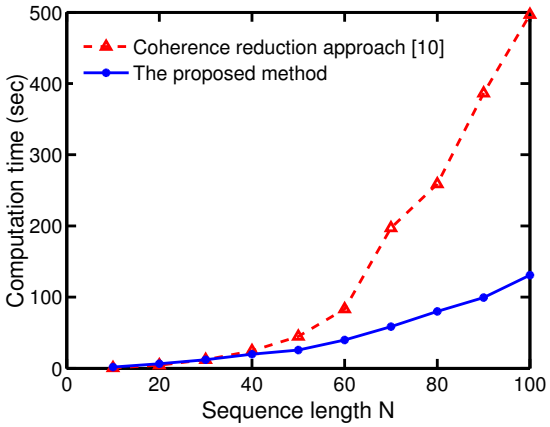

Fig. 3. Comparison of the computation times corresponding to the proposed method and the design algorithm devised in [10], for different lengths N of the transmit sequence.

Intel Core i5 CPU 750 @2.67GHz, and 8GB memory.

REFERENCES

[1] D. Donoho, "Compressed sensing," *IEEE Transactions on Information Theory*, vol. 52, no. 4, pp. 1289–1306, April 2006.

[2] E. Candès and M. Wakin, "An introduction to compressive sampling," *IEEE Signal Processing Magazine*, vol. 25, no. 2, pp. 21–30, March 2008.

[3] Y. He, X. Zhu, S. Zhuang, H. Li, and H. Hu, "Waveform optimization for compressive sensing radar imaging," in *IEEE CIE International Conference on Radar*, vol. 2. Chengdu, China: IEEE, 2011, pp. 1263–1266.

[4] Y. Yu, A. P. Petropulu, and H. V. Poor, "MIMO radar using compressive sampling," *IEEE Journal of Selected Topics in Signal Processing*, vol. 4, no. 1, pp. 146–163, 2010.

[5] W. Roberts, P. Stoica, J. Li, T. Yardibi, and F. A. Sadjadi, "Iterative adaptive approaches to MIMO radar imaging," *IEEE Journal of Selected Topics in Signal Processing*, vol. 4, no. 1, pp. 5–20, 2010.

[6] V. M. Patel, G. R. Easley, D. M. Healy Jr, and R. Chellappa, "Compressed synthetic aperture radar," *IEEE Journal of Selected Topics in Signal Processing*, vol. 4, no. 2, pp. 244–254, 2010.

[7] L. Zhang, M. Xing, C.-W. Qiu, J. Li, J. Sheng, Y. Li, and Z. Bao, "Resolution enhancement for inversed synthetic aperture radar imaging under low SNR via improved compressive sensing," *IEEE Transactions on Geoscience and Remote Sensing*, vol. 48, no. 10, pp. 3824–3838, October 2010.

[8] P. Stoica, J. Li, and M. Xue, "Transmit codes and receive filters for radar," *IEEE Signal Processing Magazine*, vol. 25, no. 6, pp. 94–109, 2008.

[9] M. Herman and T. Strohmer, "High-resolution radar via compressed sensing," *IEEE Transactions on Signal Processing*, vol. 57, no. 6, pp. 2275–2284, June 2009.

[10] J. Zhang, D. Zhu, and G. Zhang, "Adaptive compressed sensing radar oriented toward cognitive detection in dynamic sparse target scene," *IEEE Transactions on Signal Processing*, vol. 60, no. 4, pp. 1718–1729, 2012.

[11] M. Soltanalian, M. M. Naghsh, and P. Stoica, "On meeting the peak correlation bounds," *IEEE Transactions on Signal Processing*, vol. 62, no. 5, pp. 1210–1220, March 2014.

[12] M. Elad, *Sparse and redundant representations: from theory to applications in signal and image processing*. New York, NY: Springer, 2010.

[13] H. He, J. Li, and P. Stoica, *Waveform design for active sensing systems: a computational approach*. Cambridge University Press, 2012.

[14] H. He, P. Stoica, and J. Li, "Designing unimodular sequence sets with good correlations—including an application to MIMO radar," *IEEE Transactions on Signal Processing*, vol. 57, no. 11, pp. 4391–4405, 2009.

[15] M. Soltanalian, M. M. Naghsh, and P. Stoica, "A fast algorithm for designing complementary sets of sequences," *Signal Processing*, vol. 93, no. 7, pp. 2096–2102, 2013.

[16] M. Rossi, A. M. Haimovich, and Y. C. Eldar, "Spatial compressive sensing for MIMO radar," *IEEE Transactions on Signal Processing*, vol. 62, no. 2, pp. 419–430, January 2014.